JOURNAL OF SOLID STATE CHEMISTRY 46, 294–305 (1983)

Luminescence in Trilanthanumtrichlorotungstate ($La_3WO_6Cl_3$)

G. BLASSE AND G. J. DIRKSEN

Physical Laboratory, State University, P.O. Box 80.000, 3508 TA Utrecht, The Netherlands

AND L. H. BRIXNER

E. I. du Pont de Nemours and Company, Inc., Central Research and Development Department, Experimental Station, Wilmington, Delaware 19898

Received June 28, 1982

The luminescence properties of $La_3WO_6Cl_3$ are reported and discussed. The tungstate group occurs as a trigonal prismatic WO_6^{6-} complex. The blue luminescence is, for the greater part, quenched at room temperature. No energy migration occurs in this lattice. The decay times are discussed in terms of a simple molecular-orbital (MO) scheme. The luminescence of the following activating ions was studied: Mo^{6+}, Bi^{3+}, Eu^{3+}, Sm^{3+}, Ce^{3+}, and Tb^{3+}. The molybdate group produces a red emission with low efficiency. The Bi^{3+} ion induces a narrow band emission with small Stokes shift. This is interpreted using a Bi^{3+}–O^{2-}–W^{6+} charge-transfer state. Except for Ce^{3+}, the rare earth activators show luminescence, but the total transfer efficiency from tungstate to the rare-earth ions is low. This is not due to the one-step tungstate–rare-earth transfer (which is efficient), but to the localized nature of the tungstate excitation. The Eu^{3+} charge-transfer band is at very low energies.

1. Introduction

Recently Brixner *et al.* have described the crystal structure of $La_3WO_6Cl_3$ (*1*). In this structure the tungsten ion has a very remarkable trigonal prismatic coordination. Usually hexavalent tungsten is coordinated either tetrahedrally (e.g., $CaWO_4$) or octahedrally (e.g., Ba_2CaWO_6) in oxides. Since the WO_4^{2-} tetrahedron as well as the WO_6^{6-} octahedron is known to be an efficient luminescent center (*2*), it seemed interesting to investigate the luminescence properties of $La_3WO_6Cl_3$ to see whether the trigonal prismatic coordination would yield any special effects. In Ref. (*1*) the emission and excitation spectra of the luminescence of $La_3WO_6Cl_3$ have been reported; here we present a more detailed study.

It was also reported in Ref. (*1*) that several rare-earth ions show luminescence in this host lattice; for that reason we extended that investigation also. The luminescence properties of $La_3WO_6Cl_3$–U, which is an efficient orange-emitting phosphor, were described and discussed in a previous paper (*3*). Here we investigated the luminescence of the following activators: Mo^{6+} (for W^{6+}) and Ce^{3+}, Sm^{3+}, Eu^{3+}, Tb^{3+}, Bi^{3+} (for La^{3+}). The La^{3+} ions in $La_3WO_6Cl_3$ are in 10-coordination, with six O^{2-} ions on one side and four Cl^- ions on the other side (*1*).

0022-4596/83/030294-12$03.00/0

Copyright © 1983 by Academic Press, Inc.
All rights of reproduction in any form reserved.

This asymmetric coordination is similar to that of LaOCl in which the luminescence of many activators has been investigated (*4*).

2. Experimental

Samples were prepared as described in Ref. (*1*). The trivalent activators were introduced into the starting material LaOCl. Molybdenum was introduced as MoO_3 together with WO_3. Samples were checked by X-ray powder diffraction. The activator concentrations varied from 1 to 5 atomic percent.

A description of the optical instrumentation has been given before (*3*).

3. Results and Discussion

3.1. Unactivated $La_3WO_6Cl_3$

The unactivated $La_3WO_6Cl_3$ shows a weak blue emission under short wavelength ultraviolet excitation at room temperature. At lower temperatures its intensity increases considerably. Figure 1 shows the emission and excitation spectra of this luminescence at LHeT. The emission band peaks at about 445 nm, the corresponding excitation band, at 300 nm. The Stokes shift

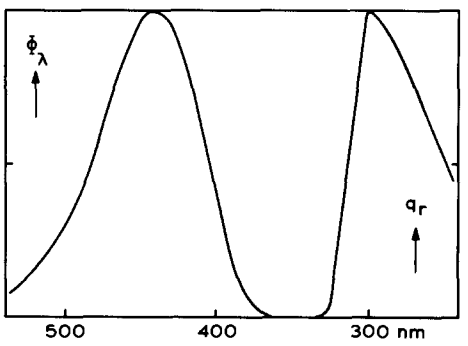

FIG. 1. Emission (left) and excitation (right) spectra of the luminescence of $La_3WO_6Cl_3$ at LHeT. Φ_λ gives the spectral radiant power per wavelength interval, and q_r the relative quantum output, both in arbitrary units.

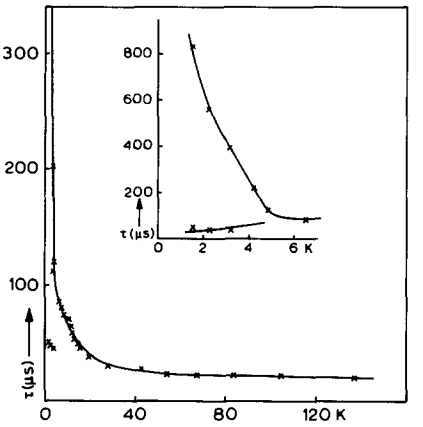

FIG. 2. Decay times (τ) of the luminescence of $La_3WO_6Cl_3$ as a function of temperature. See also text.

is about 10,500 cm^{-1}. This is a low value: for octahedral tungstate groups about 12,000 cm^{-1} has been reported; for tetrahedral tungstate groups values exceeding 15,000 cm^{-1} have been reported (*2*).

The temperature dependence of the luminescence was also measured. At 180 K the intensity had decreased to 50% of the LHeT value; at room temperature only about 5% is left. The quantum efficiency at LHeT is at least 80%.

Figure 2 presents the results of decay time measurements ($1/e$ values) on the luminescence of $La_3WO_6Cl_3$. The results are fairly complex. At very low temperatures the decay curves are not simply exponential; they can be analyzed to give two decay times. Above 5 K the decay curves are exponential yielding one value for the decay time. This does not necessarily mean that there is only one decay time. It might well be that the two decay times observed near LHeT are now of the same order of magnitude, so that we can no longer observe the difference. At still higher temperatures the decay time decreases because of temperature quenching.

The present results differ considerably from those obtained for the tetrahedral tungstate group. For the latter species we

have broader spectral bands, larger Stokes shifts, and single exponential decay times. The temperature dependence of the decay times reveals one trap level. This has been interpreted by the assumption that the emission originates from the spin–orbit split $^3T_1$ level (*2*).

On the other hand, the results for $La_3WO_6Cl_3$ show some analogy with those for the octahedral tungstate group (*2, 5, 6*). For this group the spectral bands are also narrower than for the tetrahedral tungstate groups, and the Stokes shift is about equal to that observed for the $La_3WO_6Cl_3$ luminescence. These spectral properties confirm a hypothesis made before (*2*). The W^{6+} ion is too large for a tetrahedral hole in oxides, but too small for an octahedral hole. Orgel (*7*) based an explanation of ferroelectricity upon this feature. In the antibonding excited state of the tungstate group, the W–O distance will be larger than in the ground state. This expansion will be larger in the tetrahedron, where the W^{6+} ion did not have enough space in the ground state. In the octahedron, part of this expansion can be absorbed by the space available, the central metal ion being relatively small. Obviously, this is also true for the trigonal prism. The smaller offset between the parabolas for six coordination results in narrower spectral bands and in a smaller Stokes shift.

For the octahedral group it was observed that the emission originates from two different levels which were not connected. This was not observed clearly in the spectra, because we were dealing with two broad bands with a small energy difference. However, the emission showed two decay times at all temperatures. Molecular-orbital calculations confirmed this model. The emission originates from two $^3T_1$ levels. At very low temperatures the decay times rise due to the presence of metastable levels among the spin–orbit split components of these levels.

The situation for the tungstate trigonal prism in $La_3WO_6Cl_3$ seems to be analogous. Spectrally we observe only one emission and one excitation band. At low temperatures, however, there are two decay times. It is not clear whether at higher temperatures we have two decay times which are about equal, or one decay time. The longer decay time increases if the temperature decreases, indicating a lower metastable level; the shorter decay time decreases if the temperature decreases, indicating a metastable level above the emitting level (*2*).

Unfortunately, no molecular orbital calculations on a WO_6 prism are available in the literature. It is possible to derive a simple model, applying general group-theoretical methods. The empty *d* level of the tungsten ion breaks up into three components, viz., $a_1' + e' + e''$, under the D_{3h} symmetry of the trigonal prism. According to calculations (*8*) this is the sequence of increasing energy, so that the lowest unoccupied MO has symmetry a_1'. To find the symmetry of the highest filled MO, we derived the representations of the combinations of oxygen $2p$ orbitals involved in σ and π bonding: $\Gamma_\sigma = a_1' + e' + a_2'' + e''$ and $\Gamma_\pi = a_1' + a_2' + 2e' + a_1'' + a_2'' + 2e''$. This leads to the nonbonding MOs $a_2' + a_1'' + 2a_2''$. The excited state should therefore contain $^3A_2' + {}^3A_1'' + 2{}^3A_2'' + {}^1A_2' + {}^1A_1'' + 2{}^1A_2''$. From the ground state $^1A_1'$ allowed transitions are only possible to the two $^1A_2''$ levels (z polarized). All other transitions are orbitally and/or spin forbidden. The emission is clearly a forbidden transition, since the decay times are longer than 10 μsec. Since this corresponds to a reasonable oscillator strength, we assume, following Van Oosterhout (*5, 6*), that the emission originates from the two $^3A_2''$ levels. Emission from the other two spin triplet levels is orbitally forbidden.

In this way we have found a way to explain the two decay times. Their temperature dependences at low temperatures may

be due to the spin–orbit splitting of the $^3A_2''$ levels, yielding $A_1'' + E'$. Emission from the latter sublevel is more allowed than from the former. This model explains the experimental observations. Confirmation would be possible by extended MO calculations, with measurements of the polarization of the tungstate emission and absorption on single crystals of $La_3WO_6Cl_3$.

In our approach we have neglected energy transfer between tungstate groups. That this is justified follows from our results on $La_3WO_6Cl_3$–U (*3*) and the results to be described below.

3.2. $La_3W_{1-x}Mo_xO_6Cl_3$

The molybdate group has its energy levels always at lower energies than the corresponding tungstate group. Examples of studies on molybdate-activated tungstates are $CaW_{1-x}Mo_xO_4$ (*9*) and $Y_2W_{1-x}Mo_xO_6$ (*10*). Since the molybdate trigonal prism has not been described, we studied also the molybdate group in $La_3WO_6Cl_3$. Because of its preference for tetrahedral coordination, such a trigonal molybdate prism seems to be even more exceptional than the tungstate prism.

It appeared possible to dissolve a few percent of molybdenum into the chlorotungstate. A sample with 3 atomic percent molybdenum showed only the weak blue tungstate emission at room temperature. At lower temperatures, however, a red emission is also present. Figure 3 shows the relevant emission and excitation spectra of this luminescence at LHeT. The spectral bands involved are as broad as the tungstate bands, so that they must be due to the molybdate prism.

The emission band shows a maximum at about 610 nm. The corresponding excitation band peaks at 365 nm. The Stokes shift is about 11,000 cm^{-1}, in good agreement with the value for the prismatic tungstate luminescence. The excitation spectrum was run for the longer wavelength tail of the molybdate emission, so that absolutely no tungstate emission is monitored. The presence of the tungstate excitation band in this spectrum (see Fig. 3 and compare Fig. 1) indicates energy transfer from the tungstate to the molybdate group.

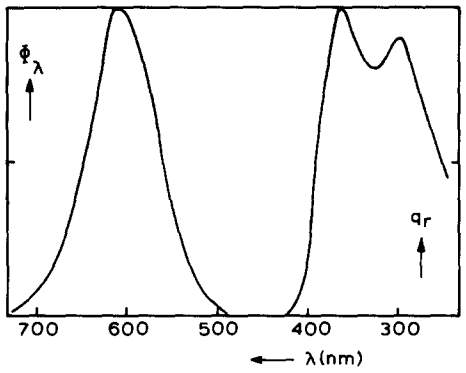

FIG. 3. Emission and excitation spectra of the molybdate luminescence of $La_3W_{0.97}Mo_{0.03}O_6Cl_3$ at LHeT. The excitation spectrum is recorded for 660-nm emission (i.e., tungstate emission absent). The excitation maximum at 300 nm is due to tungstate absorption.

At about 80 K the intensity of the molybdate luminescence has dropped to 50% of the LHeT value; at still higher temperatures it fades away gradually. The quantum efficiency of the molybdate emission is low. At LHeT it amounts to less than 5% of that of the tungstate luminescence. In view of this low efficiency we were unable to measure decay times with any accuracy. At LHeT a very rough estimate of 10 μsec was made. From this we extrapolate for the radiative decay time of the molybdate prism a value of 250 μsec.

The spectral characteristics of the trigonal, prismatic molybdate group are, therefore, very similar to those of the corresponding tungstate group, but situated at lower energies, as is to be expected (*9, 10*). The radiative decay time is considerably longer than for the tungstate group. This has been observed before and is ascribed to the weaker spin–orbit coupling constant for molybdenum (*2, 11*).

Octahedral molybdate emission has been observed for potassium oxalatomolybdate (*12*). This emission is also in the red with low efficiency. The low efficiency has been ascribed to the fact that broadband emitting levels at low energy cannot luminesce efficiently in a simple configurational coordinate model (*13, 14*). The same reasoning holds for the trigonal prismatic group.

The quantum efficiency of the tungstate emission of $La_3W_{0.97}Mo_{0.03}O_6Cl_3$ is about the same as for the sample without molybdenum. This indicates that the transfer from tungstate to molybdate group is restricted to nearest neighbors. This observation is temperature independent, which excludes energy migration in the tungstate subsystem. Similar observations were made in other molybdate-activated tungstates (*9, 10*).

3.3 $La_{3-x}Bi_xWO_6Cl_3$

Ions with s^2 configuration (Pb^{2+}, Bi^{3+}) often induce efficient luminescence in vanadates, tungstates, and related compounds. Well-known examples are $(Ca,Pb)WO_4$ (*9*) and $(Y,Bi)VO_4$ (*15, 16*). For this reason we investigated the influence of the Bi^{3+} ion on the luminescence of $La_3WO_6Cl_3$. We were able to prepare samples containing a few atomic percent of bismuth. Here we describe results for $La_{2.94}Bi_{0.06}WO_6Cl_3$. The diffuse reflection spectrum of this composition shows an additional absorption starting at about 420 nm at room temperature and extending to the tungstate absorption edge.

At room temperature we observed only the very weak blue tungstate emission under $\lambda < 300$ nm excitation. At liquid nitrogen temperature this emission is considerably more intense. No new emission has occurred. At LHeT, however, new phenomena appear. Under long wavelength excitation we observed a sharp emission band peaking at 455 nm (see Fig. 4). Although this emission band has its maximum at nearly the same position as the tungstate

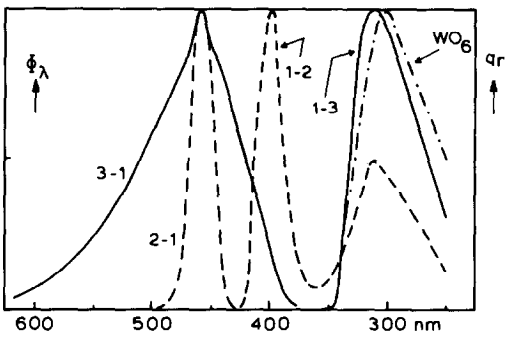

FIG. 4. Emission and excitation spectra of the luminescence of $La_{2.94}Bi_{0.06}WO_6Cl_3$ at LHeT. The 3–1 emission is for 330-nm excitation, the 2–1 emission for 400-nm excitation. The 1–2 excitation is for 460-nm emission, the 1–3 excitation is for 530-nm emission. The tungstate excitation is for 420-nm emission. The *i–j* notation relates to Fig. 6.

emission, its width is considerably narrower. This indicates that we are dealing with a new luminescent center. Under short wavelength excitation we observed the tungstate emission band. Since the two emission bands overlap, it is difficult to decide whether the emission spectrum upon tungstate excitation contains also the narrow emission band or not.

The excitation spectra depend strongly on the emission wavelength monitored. For $\lambda = 420$ nm (only tungstate emission) we find the tungstate excitation band mentioned above (300 nm). For $\lambda = 460$ nm (tungstate as well as narrow band emission) we observe two excitation bands, viz. the 300 nm tungstate band and, in addition, an excitation band with a maximum at about 400 nm (see Fig. 4). This coincides with the additional absorption in the reflection spectrum. We conclude that the presence of Bi^{3+} in $La_3WO_6Cl_3$ yields a luminescent center which gives a narrow emission band with a maximum at 455 nm. The corresponding excitation band is at 400 nm. The Stokes shift of this luminescence is, therefore, 3000 cm^{-1}.

The temperature dependence of the intensity of this emission shows that at 60 K

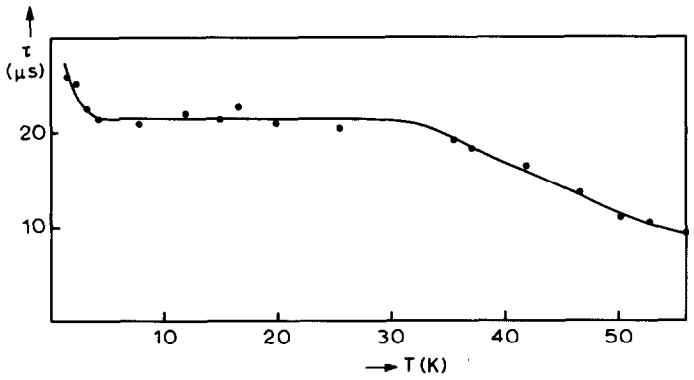

FIG. 5. Decay times of the 455-nm emission band of $La_{2.94}Bi_{0.06}WO_6Cl_3$ as a function of temperature.

the LHeT value has decreased to 50%. At 80 K the emission is quenched completely. It was possible to measure decay times of this emission under excitation into the long wavelength excitation band. All decay curves were single exponentials. Figure 5 shows the decay times as a function of temperature. There is a plateau value of some 20 μsec. At low temperatures this value increases slightly.

Returning to the excitation spectra, we find that the emission with $\lambda = 530$ nm produces a shoulder on the low-energy side of the tungstate excitation band. If we excite with 330 nm radiation, i.e., mainly into this shoulder, we observe a broad emission band on top of which occurs the narrow emission band with the 455 nm maximum. This emission band consists of the tungstate emission band and an additional broad emission band with a maximum at longer wavelength (see Fig. 4). It seems that our sample contains another luminescent center. Because of overlap with the tungstate spectral bands it is hard to provide accurate data for this center. Its emission is a broad-band with an emission maximum somewhere near 500 nm. This emission is excited in an area around 320 nm. The Stokes shift is, therefore, comparable to that of the tungstate emission. This emission is completely quenched above 80 K; it is not observed in nominally pure $La_3WO_6Cl_3$.

A discussion of the nature of the emitting centers follows. The tungstate group has been described above. An obvious possibility for the narrow-band-emitting-center is to ascribe it to the Bi^{3+} ion. Because of the s^2 configuration, the emission is then ascribed to the $^3P_{1,0} \rightarrow {}^1S_0$ transition, and the excitation band at 400 nm, to the $^1S_0 \rightarrow {}^3P_1$ transition (*15*). However, the decay time measurements do not confirm such an assignment. For the Bi^{3+} ion we expect a low-temperature decay time of several hundreds of μsec, which changes to a higher-temperature value of a few μsec (*17*). In view of the Stokes shift of 3000 cm^{-1}, this behavior should be clearly observable (*18*). In addition the Bi^{3+} spectral bands are expected at higher energies, because in LaOCl–Bi^{3+} the emission and excitation bands are both situated in the ultraviolet (*19*).

Another possibility is to ascribe the narrow band emission to a tungstate–Bi^{3+} complex, as argued before (*20*). This means that the spectral transitions are due to tungstate charge-transfer transitions in which a certain degree of $Bi^{3+}(6s^2)$-to-$W^{6+}(5d^0)$ charge-transfer character is taken into account. This reduces the Stokes shift, because of the smaller change in bonding character, as a result of the antibonding character of the s^2 configuration (*2, 21*). The case of $La_3WO_6Cl_3$–Bi is an impressive example of

this phenomenon, because the Stokes shift is only 3000 cm^{-1}. This points to a considerable amount of Bi^{3+}–W^{6+} charge transfer in the transition. The small Stokes shift, i.e., a small parabola offset, results in narrow spectral bands, in agreement with observation.

In view of the low Bi^{3+} concentration the optical transitions occur in a center to be described as Bi^{3+}–O^{2}–W^{6+}. This means that the symmetry is low. Only the spin-selection rule is still effective. Because of the strong spin–orbit coupling in Bi^{3+} and W^{6+} this rule is greatly relaxed. The experimental value agrees with this feature. The low-temperature behavior of τ vs T (Fig. 5) indicates that there exist only levels with a very weak trap depth. This indicates that the symmetry is low (compare the discussion in Section 3.1 on $La_3WO_6Cl_3$). In view of these arguments we ascribe the narrow band emission to a Bi^{3+}–O^{2-}–W^{6+} center.

We are left with another problem, viz., the low quenching temperature of this emission. For such a small Stokes shift a very high quenching temperature is to be expected, especially if the concentration of the centers is relatively low. Such high quenching temperatures have been observed, e.g., in the case of $CaWO_4$–Pb. Values up to 700 K have been reported (*2, 21*). There is an obvious explanation for the low quenching temperature of the Bi^{3+}–O^{2-}–W^{6+} center emission of $La_3WO_6Cl_3$–Bi. Note that this quenching temperature coincides with the quenching temperature of the other additional emission band. We propose that the excitation shoulder at 320 nm belongs also to this center. The configurational coordinate diagram of this center has been drawn schematically in Fig. 6.

The 455-nm emission (narrow) is ascribed to the emission 2 → 1 (small offset). The low quenching temperature is due to the presence of parabola 3 (large offset). A nonradiative return from 2 to 1 is possible via 3 with a low activation energy. Excitation into 3 yields emission from 2 and 3 as observed. Emission from 3 to 1 yields broad band emission due to the large offset. Further the quenching temperatures of the two emissions should be equal. Parabola 2 contains considerable Bi^{4+}–W^{5+} charge-transfer character (small offset). Parabola 3 originates from another configuration in which the bismuth participates considerably less. Our measurements are not accurate enough to characterize Parabola 3 any further. These results confirm the conclusion made elsewhere (*2*) that centers consisting of s^2 and closed-shell transition metal ions deserve further study.

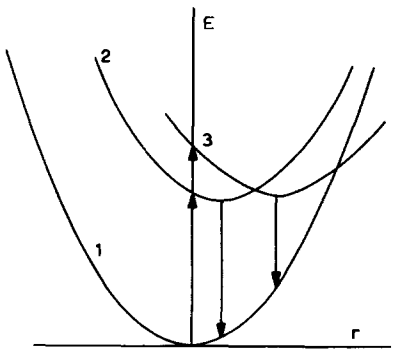

FIG. 6. Schematical configurational coordinate diagram for the Bi^{3+}–O^{2-}–W^{6+} center (see text).

3.4. $La_3WO_6Cl_3$–Eu

A number of tungstates are suitable host lattices for Eu^{3+} activation, in the sense that excitation into the tungstate group results in efficient Eu^{3+} emission (see, e.g., Ref. (*10*)). For this reason we investigated the luminescence properties of Eu^{3+}-activated $La_3WO_6Cl_3$. Unfortunately, such efficient emission was not observed. Here we will discuss the composition with 1 atomic percent europium, viz., $La_{2.97}Eu_{0.03}WO_6Cl_3$.

At room temperature there is a rather weak emission consisting mostly of tungstate emission if excitation involves the tungstate group. The excitation spectrum of

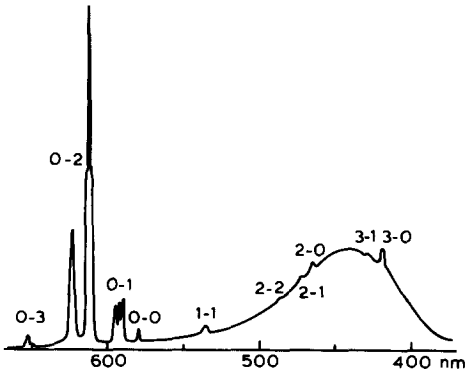

FIG. 7. The emission spectrum of $La_{2.97}Eu_{0.03}WO_6Cl_3$ at LHeT under 322-nm excitation. The J'–J notation relates to the transitions $^5D_{J'}$–^7F_J.

the red europium emission contains a broadband peaking at about 340 nm. This band is at longer wavelength than the tungstate excitation band which is practically absent. This shows that at room temperature there is practically no tungstate to Eu^{3+} transfer. Similar results were described before (Fig. 11 of (*1*)).

At LHeT the emission intensity is much higher due to an increased tungstate emission intensity. Excitation in the tungstate excitation band (e.g., $\lambda = 300$ nm) yields an emission spectrum in which the Eu^{3+} lines are scarcely visible. Their contribution is 1% or less. For excitation with $\lambda = 322$ nm we see much more Eu^{3+} emission (see Fig. 7). Note that emission originates not only from $^5D_0$, but also from $^5D_1$, $^5D_2$, and $^5D_3$. The excitation spectrum of the Eu^{3+} emission from $^5D_0$ is given in Fig. 8. Note the broadband in addition to the characteristic Eu^{3+} lines. This band is not the tungstate excitation band.

The emission spectrum under tungstate excitation was also measured as a function of temperature. The tungstate emission band decreases as described above for the undoped tungstate. The Eu^{3+} emission remains as weak as it is at LHeT. This confirms the result mentioned above that the tungstate excitation energy does not become mobile at higher temperatures.

Let us first discuss the Eu^{3+} emission. The site symmetry of La^{3+} in $La_3WO_6Cl_3$ is very low, viz. C_s (*1*). For this site symmetry the degeneracy of all levels is lifted and all transitions are allowed. In Fig. 7 it can be seen that for $^5D_0$–$^7F_0$ and $^5D_0$–$^7F_1$ the expected number of lines is observed (1 and 3, respectively). Under the present resolution we find at least 4 and 7 lines for $^5D_0$–$^7F_2$ and $^5D_0$–$^7F_4$ (theoretically 5 and 9, respectively); thus, Eu^{3+} resides on the La^{3+} site in $La_3WO_6Cl_3$.

The broadband in the Eu^{3+} excitation spectrum (Fig. 8) cannot be due to the tungstate group. It corresponds to the Eu^{3+}–$O^{2-}(Cl^-)$ charge-transfer transition. The maximum (at LHeT about 330 nm) is not necessarily the absorption maximum, because the excitation band shrinks on the short wavelength site due to tungstate absorption which is not converted into Eu^{3+} emission. Nevertheless we can safely conclude that this charge-transfer transition is at relatively low energy. For LaOCl–Eu^{3+} 300 nm has been reported as the maximum of the Eu^{3+} charge-transfer band at room temperature (*22*). In the oxychloride this

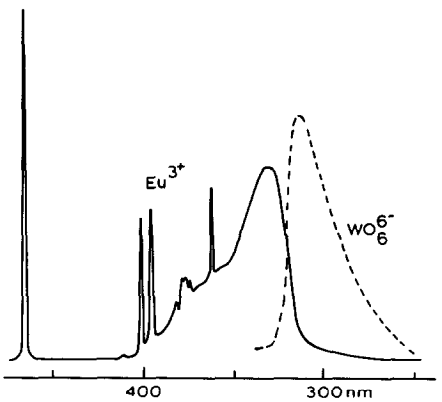

FIG. 8. The excitation spectrum of the $^5D_0$ emission of Eu^{3+} in $La_{2.97}Eu_{0.03}WO_6Cl_3$ at LHeT. The excitation spectrum of the tungstate emission is given by the broken line.

band starts at about 350 nm, in our case, at 410 nm (300 K). In oxides its maximum is usually around 250 nm and only seldom below 300 nm (*23*). Hoefdraad has noted that the charge-transfer band moves to lower energy if the coordination of the Eu^{3+} ion is higher (*23*). We therefore assume that the 10 coordination of Eu^{3+} in $La_3WO_6Cl_3$ is mainly responsible for the low-energy position of the Eu^{3+} charge-transfer band in $La_3WO_6Cl_3$.

At the same time it should be realized that a low position of this band promotes nonradiative transitions in the Eu^{3+} ion (*24*). In $LaAlO_3$–Eu^{3+}, for example, the charge-transfer absorption maximum is at 315 nm and the Eu^{3+} quantum efficiency is 30% (*25*). It cannot be excluded, therefore, that the low Eu^{3+} emission intensity is partly due to nonradiative losses. This is especially true for the room temperature results.

However, even if the present results are corrected for nonradiative losses in the Eu^{3+} ion, the amount of energy transfer to Eu^{3+} is low. The situation is comparable to that in $La_3WO_6Cl_3$–U (*3*). First we note that the excitation energy does not migrate within the tungstate sublattice. Probably the relaxed excited state of the tungstate group is too far out of resonance, so that the probability for tungstate–tungstate transfer cannot compete with radiative tungstate decay (*26*). If we take into account one-step energy transfer between the tungstate group and Eu^{3+} ions on nearest La^{3+} neighbor sites only, we find for our sample that 91% of the emission should be from the tungstate (viz., 0.99^9) and 9% from the Eu^{3+} ion.

Since the tungstate emission overlaps even with the Eu^{3+} charge-transfer state there is no reason why the $WO_6^{6-} \rightarrow Eu^{3+}$ transfer should be inefficient. We suppose that under the sample preparation conditions a slight amount of reduction occurs which reduces part of the europium ions to the divalent state. Note that the sample in Ref. (*1*) with about the same nominal europium concentration shows extensive $^5D_3$, $^5D_2$, and $^5D_1$ emission which points to a much lower Eu^{3+} concentration than in our sample. These samples were made in different laboratories and, therefore, under slightly different circumstances. Reduction would also lower the U^{6+} concentration of our samples $La_3WO_6Cl_3$–U (*3*). We assume therefore that the low fraction of Eu^{3+} emission in our samples is due to trivial reasons. If we assume that the experimental fraction is 1% and that 50% of the Eu^{3+} excitation energy is lost nonradiatively, we estimate that 25% of the europium is present in the trivalent state.

3.5. $La_3WO_6Cl_3$–Sm

In view of the results with the Eu^{3+}-activated samples which were complicated for several reasons, we also prepared and investigated Sm^{3+}-activated samples, because no complications with low-lying charge-transfer states are to be expected and samarium is more difficult to reduce to the divalent state than europium. Here we present results for the composition $La_{2.98}Sm_{0.02}WO_6Cl_3$.

At room temperature the luminescence under tungstate excitation has medium to weak intensity; 60% of this emission consists of Sm^{3+} emission (the well-known, characteristic lines in the red) and 40% of tungstate emission. The Sm^{3+} excitation spectrum contains the Sm^{3+} lines and the tungstate excitation band. In contrast to the Eu^{3+} case, we can conclude that energy transfer occurs from the tungstate group to Sm^{3+}.

At LHeT the tungstate emission becomes much stronger. The emission spectrum under tungstate excitation consists mainly of tungstate emission (93%); the Sm^{3+} lines contribute for 7% to the total emission intensity. The Sm^{3+} excitation spectrum does not change very much.

These results can be simply explained by assuming tungstate → Sm^{3+} transfer between nearest neighbors only, neglecting tungstate → tungstate transfer at all temperatures and remembering the thermal quenching of the tungstate luminescence (Section 3.1). At LHeT we expect in this model $(1 - \frac{1}{3} \cdot 0.02)^9 = 94\%$ tungstate emission and 6% Sm^{3+} emission, in excellent agreement with experiment. At 300 K about 5% of the tungstate emission should remain, so that about 60% of the total emission should indeed be Sm^{3+}. Here we have assumed that also at 300 K the probability for tungstate → Sm^{3+} transfer exceeds the radiative and nonradiative probabilities of the tungstate group; this seems to be correct. Since the radiative probability at room temperature is about 10^5 sec^{-1}, the nonradiative probability is about $2 \cdot 10^6$ sec^{-1}. The transfer probability must, therefore, exceed 10^7 sec^{-1}, in good agreement with other observations (see, e.g., (*27*)).

3.6. $La_3WO_6Cl_3$–Ce

Whereas Sm^{3+} and Eu^{3+} are rare-earth ions which tend to become divalent, Ce^{3+} and Tb^{3+} have a tendency to become tetravalent. It seemed interesting to investigate their properties in $La_3WO_6Cl_3$ also. In this section we report on the Ce^{3+} ion. Samples of $La_3WO_6Cl_3$–Ce are yellow in color. A representative reflection spectrum is given in Fig. 9.

This spectrum shows the tungstate absorption edge around 310 nm and a long tail without structure into the visible. It seems quite improbable that this absorption is due to the $4f \rightarrow 5d$ absorption bands of the Ce^{3+} ion, because these are usually situated at higher energy in oxides and show structure as a result of crystal-field splitting of the $5d$ level. The present spectrum shows a striking analogy with that of $SrTiO_3$–Ce (*28*). Strong arguments have been given there to assign this absorption to a $Ce^{3+} \rightarrow Ti^{4+}$ charge-transfer transition. We assume that

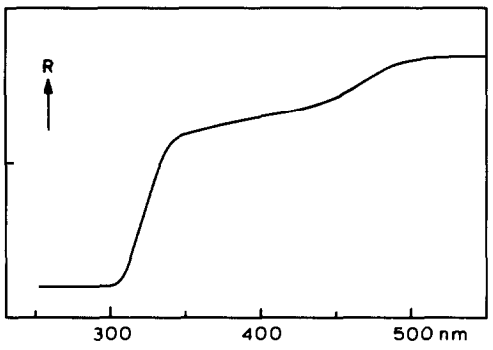

FIG. 9. The diffuse reflection spectrum of $La_{2.97}Ce_{0.03}WO_6Cl_3$ at room temperature.

the same holds here, i.e., that the absorption tail is due to a $Ce^{3+} \rightarrow W^{6+}$ charge-transfer transition.

Samples $La_3WO_6Cl_3$:Ce do not show any luminescence under ultraviolet or visible excitation, not even at LHeT. The charge-transfer state Ce^{4+}–W^{5+} seems to decay nonradiatively, as argued before in another context (*29*). Any Ce^{3+} emission, to be expected in the ultraviolet or blue spectral region, will be picked up by this charge-transfer transition and quenched in this way.

3.7. *$La_3WO_6Cl_3$–Tb*

Finally we consider the luminescence of Tb^{3+} ions in $La_3WO_6Cl_3$. Several samples were prepared and results at room temperature were given before (*1*). Here we report in more detail on samples with composition $La_{3-x}Tb_xWO_6Cl_3$ ($x = 0.03$ and 0.15). The sample with $x = 0.15$ shows efficient green Tb^{3+} emission at LHeT and room temperature. At RT the tungstate contribution to the total emission is 5% or less, but at LHeT it is 50%, if excitation is into the tungstate group. For the $x = 0.03$ sample, these values are 20 and 89%, respectively (see also Fig. 10). Using the simple model described above, the calculated values are 8 and 63% for $x = 0.15$, and 33 and 91% for $x = 0.03$, respectively. This is in good agreement with experiment if we take the accu-

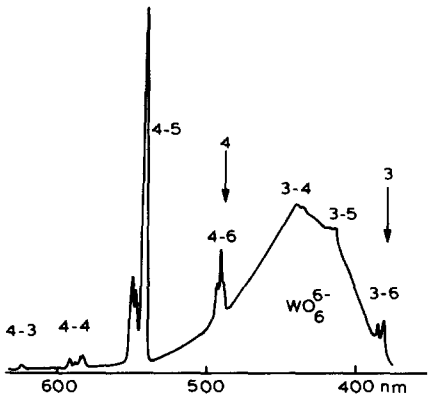

FIG. 10. The emission spectrum of $La_{2.97}Tb_{0.03}WO_6Cl_3$ at LHeT under excitation into the tungstate group. The J–J' notation is similar to that of Fig. 7. The arrows indicate the position of the lowest levels of $^5D_3$ and $^5D_4$

racy of the experiment and the simplicity of the model into account.

It is interesting to look at the ratio of the $^5D_3$ and $^5D_4$ emissions of these two samples under different excitations at LHeT (see Table I). With increasing Tb^{3+} concentration the $^5D_3$ emission is quenched as is well known (see also Ref. (*1*)). Under excitation into the $^5D_3$ level the amount of $^5D_3$ emission is much higher than under tungstate excitation. The reason for this is that the emission band of the tungstate group overlaps more favorably with the $^5D_4$ than with the $^5D_3$ level, so that the $^5D_4$ level is fed preferentially in the tungstate–Tb^{3+} energy transfer process. This has been indicated in Fig. 10 which shows the emission spectrum of $La_{2.97}Tb_{0.03}WO_6Cl_3$ under tungstate excitation and the position of the $^5D_3$ and $^5D_4$ levels as observed from the Tb^{3+} excitation and emission spectra.

TABLE I

RATIO OF THE $^5D_3$ TO $^5D_4$ EMISSION INTENSITIES AT LHeT FOR $La_{3-x}Tb_xWO_6Cl_3$ UNDER DIFFERENT EXCITATIONS

	$^5D_3/^5D_4$	
	$x = 0.03$	$x = 0.15$
Tungstate excitation	0.05	0.02
Tb^{3+} $^5D_3$ excitation	0.35	0.15

From the ratio of the Tb^{3+} and tungstate contributions to the total emission, we have to conclude that the energy transfer from the tungstate group to the Tb^{3+} ion has a probability which is not lower than in the case of Eu^{3+} and Sm^{3+}. This is rather exceptional (*30*). Usually strong quenching occurs due to charge-transfer states of the type Tb^{4+}–W^{5+} (*29*). For Ce^{3+} these were even observed directly in the reflection spectrum (see above). A possible explanation might be a relatively small offset of the charge-transfer state, but we have no proof for this. Our observations show clearly that there is no general reason why energy transfer from the tungstate group to the Tb^{3+} ion should not occur.

Acknowledgment

The authors are indebted to Mr. G. Bokkers who performed the decay time measurements.

References

1. L. H. BRIXNER, H. Y. CHEN, AND C. M. FORIS, *J. Solid State Chem.* **44,** 99 (1982).
2. G. BLASSE, *Struct. Bonding (Berlin)* **42,** 1 (1980).
3. G. BLASSE, G. J. DIRKSEN, AND L. H. BRIXNER, *J. Solid State Chem.* **44,** 162 (1982).
4. See for a review and an original report a.o. L. H. BRIXNER, J. F. ACKERMAN, AND C. M. FORIS, *J. Lumin.* **26,** 1 (1981).
5. A. B. VAN OOSTERHOUT, *Phys. Status Solidi* (a) **41,** 607 (1977).
6. A. B. VAN OOSTERHOUT, *J. Chem. Phys.* **67,** 2412 (1977).
7. L. E. ORGEL, "An Introduction to Transition-Metal Chemistry," p. 174, Methuen, London (1960).
8. R. HUISMAN, R. DE JONGE, C. HAAS, AND F. JELLINEK, *J. Solid State Chem.* **3,** 60 (1971).
9. F. A. KRÖGER, "Some Aspects of the Luminescence of Solids," Elsevier, Amsterdam (1948).

10. G. BLASSE AND A. BRIL, *J. Chem. Phys.* **45,** 2350 (1966).
11. J. A. GROENINK, C. HAKFOORT, AND G. BLASSE, *Phys. Status Solidi A* **54,** 477 (1979).
12. G. BLASSE, G. J. DIRKSEN, AND H. SAUTEREAU, *Chem. Phys. Lett.* **78,** 234 (1981).
13. K. C. BLEIJENBERG AND G. BLASSE, *J. Solid State Chem.* **28,** 303 (1979).
14. G. BLASSE, *in* "Radiationless Processes" (B. Di Bartolo, Ed.), p. 287, Plenum, New York (1980).
15. G. BLASSE AND A. BRIL, *J. Chem. Phys.* **48,** 217 (1968).
16. R. MONCORGÉ AND G. BOULON, *J. Lumin.* **18/19,** 376 (1979).
17. G. BOULON, C. PEDRINI, M. GUIDONI, AND CH. PANNEL, *J. Phys. (Paris)* **36,** 267 (1975).
18. G. BLASSE AND A. C. VAN DER STEEN, *Solid State Commun.* **31,** 993 (1979).
19. A. WOLFERT AND G. BLASSE, to be published.
20. Chap 4 in (*2*).
21. J. A. GROENINK AND G. BLASSE, *J. Solid State Chem.* **32,** 9 (1980).
22. G. BLASSE AND A. BRIL, *J. Chem. Phys.* **46,** 2579 (1967).
23. H. E. HOEFDRAAD, *J. Solid State Chem.* **15,** 175 (1975).
24. G. BLASSE, *J. Chem. Phys.* **45,** 2356 (1966); **51,** 3529 (1969).
25. G. BLASSE, A. BRIL, AND J. A. DE POORTER, *J. Chem. Phys.* **53,** 4450 (1970).
26. R. C. POWELL AND G. BLASSE, *Struct. Bonding* **42,** 43 (1980).
27. G. BLASSE AND G. J. DIRKSEN, *J. Solid State Chem.* **42,** 163 (1982).
28. G. BLASSE AND G. J. DIRKSEN, *J. Solid State Chem.* **37,** 390 (1981).
29. R. G. DE LOSH, T. Y. TIEN, E. F. GIBBINS, P. J. ZACMANIDES, AND H. L. STADLER, *J. Chem. Phys.* **53,** 681 (1970).
30. G. BLASSE AND A. BRIL, *Philips Res. Rep.* **22,** 481 (1967).